Analytical Description of Extension, Torque, and Supercoiling Radius of a Stretched Twisted DNA

Sébastien Neukirch
CNRS, UMR 7190, Institut Jean Le Rond d'Alembert, F-75005 Paris, France
UPMC Université Paris 06, UMR 7190, Institut Jean Le Rond d'Alembert, F-75005 Paris, France

John F. Marko
Department of Physics and Astronomy and Department of Molecular Biosciences, Northwestern University, Evanston, Illinois 60208, USA

(Received 14 December 2010; published 1 April 2011)

We study the mixture of extended and supercoiled DNA that occurs in a twisted DNA molecule under tension. Closed-form asymptotic solutions for the supercoiling radius, extension, and torque of the molecule are obtained in the high-force limit where electrostatic and elastic effects dominate. We demonstrate that experimental data obey the extension and torque scaling laws apparent in our formulas, in the regime where thermal fluctuation effects are quenched by applied force.

DOI: 10.1103/PhysRevLett.106.138104 PACS numbers: 87.14.gk, 82.35.Rs, 87.15.A−, 87.15.La

Experiments on stretched, supercoiled DNA primarily measure the extension of the molecule as a function of its twisting or, more precisely, as a function of change in double helix linking number Lk [1]. Past the threshold for buckling of the molecule, one enters a mixed-phase regime where part of the molecule is extended and part of the molecule is plectonemically supercoiled; in this regime the extension depends linearly on the linking number precisely because one is in a regime of two-phase coexistence [2,3].

Although the origin of the linear dependence is understood [2,4], the slopes of the extension versus linking number curves are not understood analytically. It is of broad interest to understand the slopes since, in addition to being practically useful to predict the amount of length absorbed into plectonemic supercoiling, they contain information about the interplay of external force applied to the molecule with interactions between the tightly juxtaposed DNA double helices in the plectonemic region (primarily electrostatic in the regime of interest here) [5]. Below, we analyze the parts of the "standard model" of DNA supercoiling relevant to the high-force limit. We obtain asymptotic formulas describing that limit, for the dependence of the extension versus linking number slopes and DNA torque on force and salt concentration, and we show that experimental data obey the scaling behavior implicit in our results in the high-force limit. Analytical formulas for the plectonemic supercoil radius and angle are predicted for future experiments.

We write the free energy of a DNA molecule subject to applied torque and force in the regime where extended and plectonemically supercoiled DNA are in mechanical coexistence [3,4,6,7]. The total molecule length L is partitioned between the two "phases": (i) a plectonemic phase of length ℓ, where the filament has bending rigidity A and torsional rigidity C and adopts a superhelical shape of radius r and angle α, and (ii) an extended wormlike-chain phase of length $L - \ell$; see Fig. 1. The free energy of the extended phase is described in terms of the free energy per length of the untwisted molecule $g(f) = f - k_B T(f/A)^{1/2} + \cdots$ [8], plus a twist energy using a twist modulus that includes effects of writhing fluctuations: $C_s(f) = C[1 - (C/4A)k_B T/(Af)^{1/2}]$ [6]. The free energy of the plectonemic phase is that of two superhelices wrapped around each other with electrostatic interactions. The interaction energy $U(r)$ is that of two straight charged cylinders with a center axis separated by a distance of $2r$, in the Debye-Huckle approximation of the Poisson-Boltzmann equation. For the double helix where two negative charges appear for each base pair, this suggests the use of a linear charge density (in electron charge units) of $\nu = 1/b$, where $b = 0.17$ nm is half of the 0.34 nm spacing of successive base pairs along DNA. However, an

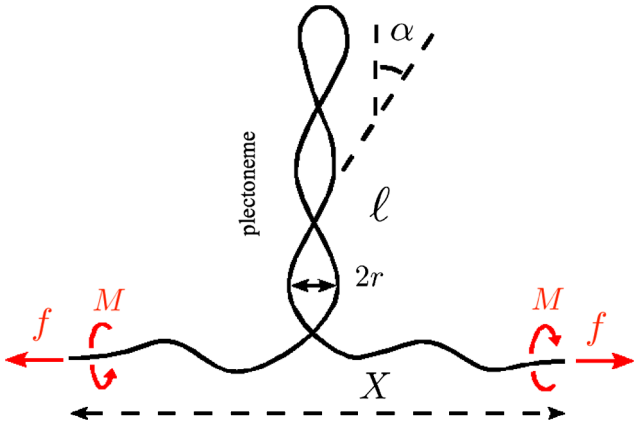

FIG. 1 (color online). Supercoiled DNA under force and torque. Molecule length is partitioned between two phases: an extended phase and a plectonemic phase where strong self-interaction occurs.

effective charge is introduced to cope with two effects: (i) the fact that this charge is distributed on the surface of the cylindrical double helix of radius $a = 1$ nm rather than on its center axis and (ii) the asymptotics of the linear and nonlinear solutions of the Poisson-Boltzmann equation have to match for large separation distances. The effective charge is

$$\nu = \frac{1}{b}\frac{1}{\gamma(L_B, b, \kappa_D a)}\frac{1}{\kappa_D a K_1(\kappa_D a)}, \quad (1)$$

where L_B is the Bjerrum length in water, κ_D^{-1} the Debye length, and $K_n(x)$ the nth modified Bessel function of the second kind [9,10]. From Table III of Ref. [9], the parameter γ is computed to be $\gamma = (1.64, 1.44, 1.27, 1.14)$ at salt concentrations $(50, 100, 200, 500)$ mM and for $T = 296.5$ K and $L_B = 0.7$ nm. The interaction potential in the plectoneme is [3,11]

$$U(r) = k_B T \nu^2 L_B K_0(2\kappa_D r), \quad (2)$$

where both κ_D and ν depend on the salt concentration. We neglect confinement entropy [3] in the interaction potential for two reasons: (i) It is important for low forces and we presently focus on the moderate- to high-force regime; (ii) our focus is on an analytical solution so we consider a simple one-term $U(r)$ (similarly, no dependence of U on superhelical angle α is considered here). The bending energy, given by the integral of the curvature squared of the molecule center line in the superhelical configuration, is a function of the superhelical radius r and angle α. By adding together electrostatic, bending, and twisting energy terms, the total free energy is

$$\mathcal{F}(\alpha, r, \lambda_s, \tau_p, \ell) = -g(L-\ell) + \frac{1}{2}C_s\lambda_s^2(L-\ell) + \left[\frac{1}{2}C\tau_p^2 + \frac{1}{2}A\frac{\sin^4\alpha}{r^2} + U(r)\right]\ell, \quad (3)$$

where $\lambda_s = 2\pi\Delta\mathrm{Lk}_s/(L-\ell)$ is the linking angle density in the stretched part of the DNA ($\Delta\mathrm{Lk}_s$ is the excess linking number of the extended region) and $\tau_p = 2\pi\Delta\mathrm{Tw}_p/\ell$ is the twist angle density in the plectonemic DNA ($\Delta\mathrm{Tw}_p$ is the excess twist in the plectoneme region). Once force and ΔLk are specified, the remaining variables are determined by minimization of Eq. (3) subject to the constraint

$$\Delta\mathrm{Lk} = \Delta\mathrm{Tw} + \mathrm{Wr} = \frac{1}{2\pi}\left(\lambda_s(L-\ell) + \tau_p\ell + \frac{\sin 2\alpha}{2r}\ell\right), \quad (4)$$

where ΔLk is the number of turns introduced into the DNA relative to the relaxed double helix linking number Lk_0 (i.e., $\Delta\mathrm{Lk} = \mathrm{Lk} - \mathrm{Lk}_0$). The constraint on ΔLk is handled by using a Lagrange multiplier M, i.e., by minimizing $\mathcal{G} = \mathcal{F} - 2\pi M(\Delta\mathrm{Tw} + \mathrm{Wr} - \Delta\mathrm{Lk})$. Equilibrium values of the six variables λ_s, τ_p, α, ℓ, r, and M follow from solving $\boldsymbol{\nabla}\mathcal{G} = 0$, where $\boldsymbol{\nabla} = (\partial/\partial\lambda_s, \partial/\partial\tau_p, \partial/\partial\alpha, \partial/\partial\ell, \partial/\partial r, \partial/\partial M)$. The equilibrium value of M is the torque in the DNA.

These nonlinear equations, when solved numerically, yield multiple solutions with either $\ell = 0$ or $\ell \neq 0$. We here focus on the stable solution having $\ell > 0$, which exists as soon as ΔLk is large enough [7]. The values of α, r, λ_s, τ_p, and M in this solution do not depend on ΔLk, and the value of ℓ varies linearly with ΔLk [7]. A consequence is that the mean extension $\langle X\rangle = -\partial\mathcal{G}/\partial f$ decreases linearly with ΔLk: As linking is added, more and more contour length passes from the extended phase to the plectonemic phase of the molecule. Figure 2 shows that the slopes $q := \partial\langle X\rangle/\partial\Delta\mathrm{Lk}$ from the experiment (data from Fig. 3 inset of Ref. [1]) are described well by this theory for four different salt concentrations (50, 100, 200, and 500 mM). Similarly, experimental and theoretical torques are in good accord (Fig. 3).

We now extract the leading scaling behavior for the slope q and the torque M from the full equations, in the high-force limit. We first approximate $C_s(f) \simeq C$, which reduces the equilibrium equations $\boldsymbol{\nabla}\mathcal{G} = 0$ to

$$-A\frac{\sin^4\alpha}{r^3} + U'(r) + M\frac{\sin 2\alpha}{2r^2} = 0, \quad (5a)$$

$$2A\frac{\sin^3\alpha\cos\alpha}{r^2} - M\frac{\cos 2\alpha}{r} = 0, \quad (5b)$$

$$g + \frac{1}{2}A\frac{\sin^4\alpha}{r^2} + U(r) - M\frac{\sin 2\alpha}{2r} = 0. \quad (5c)$$

Equations (5a) and (5c) are used to eliminate M, yielding

$$\sin^4\alpha = 2\left(\frac{gr^2}{A} + \frac{Ur^2}{A} + \frac{U'r^3}{A}\right). \quad (6)$$

Then multiplying Eq. (5b) by $\sin 2\alpha$ and Eq. (5a) by $\cos 2\alpha$ and summing, we obtain

$$\frac{U'r^3}{A} = -\frac{\sin^4\alpha}{1 - 2\sin^2\alpha}. \quad (7)$$

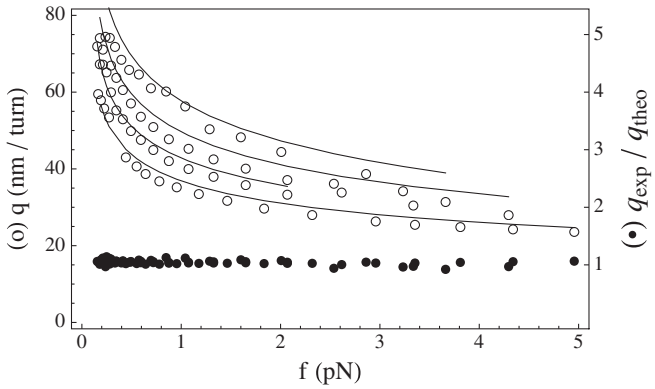

FIG. 2. Comparison of experimental and theoretical slopes as a function of the applied force, for 50, 100, 200, and 500 mM salt (top to bottom): (a) experimental data from Ref. [1] (circles); (b) theoretical solution of the full equations $\boldsymbol{\nabla}\mathcal{G} = 0$ (continuous lines); (c) ratio of the experimental slopes to the formula in Eq. (16) (filled circles). Experimentally given values of $A/kT = 46, 47, 44, 45$ nm and $C/kT = 94$ nm were used.

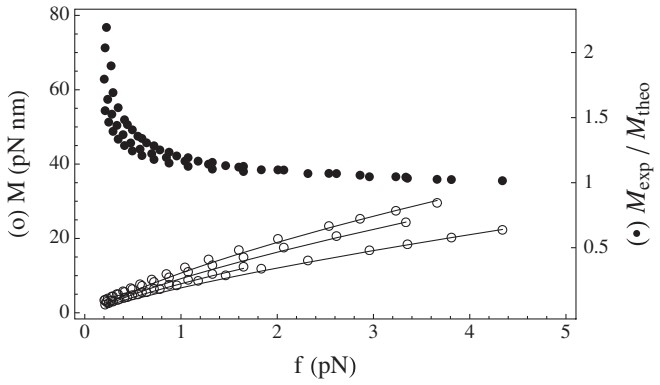

FIG. 3. Comparison of experimental and theoretical torques as a function of the applied force for 50, 100, 200, and 500 mM salt: (a) experimental data from Ref. [1] (circles); (b) theoretical solution of the full equations $\nabla\mathcal{G} = 0$ (continuous lines); (c) ratio of the experimental torque to the formula in Eq. (17) (filled circles). Experimentally given values of $A/kT = 46, 47, 44, 45$ nm and $C/kT = 94$ nm were used.

The variable α can then be eliminated from Eqs. (6) and (7) to yield one equation for the one variable r:

$$\frac{U'r^3}{A}\left[1-2\sqrt{2\left(\frac{gr^2}{A}+\frac{Ur^2}{A}+\frac{U'r^3}{A}\right)}\right] + 2\left(\frac{gr^2}{A}+\frac{Ur^2}{A}+\frac{U'r^3}{A}\right)=0. \quad (8)$$

We introduce the dimensionless variable $x := 2\kappa_D r$. In the regime of moderate to large x and of low to moderate α, the leading order of Eq. (8) is $\frac{gr^2}{A}+\frac{Ur^2}{A}+\frac{3}{2}\frac{U'r^3}{A}=0$, or

$$\sqrt{x}e^{-x}[1-1/(6x)] = 1/K \quad \text{with } K := \sqrt{9\pi/8}\nu^2 L_B k_B T/g(f) \quad (9)$$

$$\text{or } f(x) = x - \tfrac{1}{2}\log x - \log[1-1/(6x)] - \log K = 0, \quad (10)$$

where we have used $K_0(x) \simeq [\pi/(2x)]^{1/2}e^{-x}$ for large x. The approximate solution is $x_0 = \mathrm{Log}K$. Taking the first-order Newton-Raphson estimate of the root $x \simeq x_0 - \frac{f(x_0)}{f'(x_0)}$ yields

$$x = 2\kappa_D r \simeq \mathrm{Log}K + \frac{\mathrm{Log}(\mathrm{Log}K)}{2-1/\mathrm{Log}K}. \quad (11)$$

Once r is known, α is computed from Eq. (7):

$$\alpha = \arcsin\sqrt{\frac{U'r^3}{A}+\sqrt{\left(\frac{U'r^3}{A}\right)^2-\frac{U'r^3}{A}}} \quad (12)$$

and M from Eq. (5b):

$$M = \frac{2A}{r}\frac{\sin^3\alpha\cos\alpha}{\cos 2\alpha}. \quad (13)$$

Equations (11) and (12) yield, at lowest order,

$$r \simeq \bar{r} := (2\kappa_D)^{-1}\mathrm{Log}K \quad \text{and} \quad \alpha \simeq \bar{\alpha} := [2\bar{r}^2 g(f)/(3A)]^{1/4}. \quad (14)$$

We note that although our approximation always leads to a solution, this is not the case for the full equations $\nabla\mathcal{G} = 0$. For the full equations, there are two r solutions at low forces, and no solutions beyond a force threshold (we plot only the solution with the largest r value, which can be shown to be stable). The force threshold for disappearance of the stability of the large-r solution is salt-dependent and can be as low as 3 pN at low salt (5 mM Na^+); at forces beyond this threshold, the electrostatic interaction cannot support the plectoneme, which will collapse in radius down to $r \approx 1$ nm, with the two DNAs in close contact. This could explain the observations of plectoneme collapse of Ref. [12] and suggests that collapse transitions might be observable in single-DNA experiments. We note that once in the collapsed configuration, if one were to decrease the force, hysteresis of the collapsed state would be observed. We are analyzing this collapse phenomenon in more detail at present and will discuss it in a forthcoming paper.

Our formulas provide insight into the dependence of the slope q on force and salt concentration observed experimentally [1]. We compute $q := \partial\langle X\rangle/\partial\Delta\mathrm{Lk} = -\partial^2\mathcal{G}/(\partial f\partial\Delta\mathrm{Lk})$ neglecting $C_s'(f)$ (valid for large force) and taking $\lambda_s \simeq \tau_p$:

$$q \simeq g'(f)\frac{4\pi r}{\sin 2\alpha} \simeq 2\pi g'(f)\frac{r}{\alpha}\left(1+\frac{2}{3}\alpha^2\right). \quad (15)$$

Using Eq. (14), we arrive at

$$q \simeq 6^{1/4}\pi A^{1/4}\kappa_D^{-1/2}\frac{g'(f)}{g(f)^{1/4}} \times\sqrt{\mathrm{Log}\left[\sqrt{9\pi/8}\nu^2 L_B k_B T/g(f)\right]}\left(1+\frac{2}{3}\bar{\alpha}^2\right), \quad (16)$$

which gives the salt and force dependence of the slope of a hat curve in a supercoiling experiment. Figure 2 shows experimental slopes divided by this theoretical prediction; the ratio is nearly 1 with only a small variation with force and salt concentration, indicating that the experimental data closely follow this functional form.

We now examine the DNA torque M; Taylor expansion of (13) for small α yields $M \simeq \frac{2A}{r}\alpha^3(1+\frac{3}{2}\alpha^2)$. Using (14), we obtain the following approximate formula for M:

$$M \simeq (32/27)^{1/4}A^{1/4}\kappa_D^{-1/2}g(f)^{3/4} \times\sqrt{\mathrm{Log}\left[\sqrt{9\pi/8}\nu^2 L_B k_B T/g(f)\right]}\left(1+\frac{3}{2}\bar{\alpha}^2\right). \quad (17)$$

In Fig. 3, experimental torque values are divided by this theoretical prediction, and we see that, when f is large enough, the ratio is near 1, with only a small variation with f or salt concentration. As for the slopes q, the experimental data for M closely follow this functional form, for a sufficiently large force.

For forces in the range $0.25\ \mathrm{pN} \le f \le 5\ \mathrm{pN}$ and salt concentrations between 50 and 500 mM, we checked the

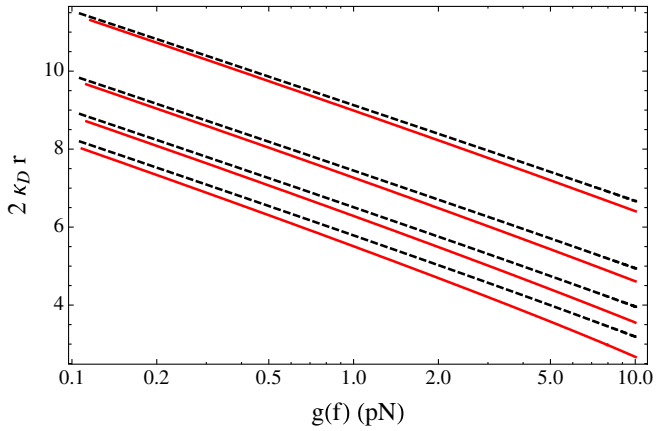

FIG. 4 (color online). Supercoiling radius as a function of the force function $g(f)$, computed with (a) the full nonlinear equations $\nabla\mathcal{G} = \mathbf{0}$ (plain lines, red); (b) the formula in Eq. (11) (dashed lines, black) for the four salt concentrations 50, 100, 200, and 500 mM (top to bottom). The separation of the curves at high force is due to the nonlinearities of $\nabla\mathcal{G} = \mathbf{0}$, which are omitted in Eq. (11).

accuracy of formulas (14), (16), and (17) against the solution of the full equations $\nabla\mathcal{G} = 0$ and found that the relative error was always below 13% (see [13]). Similarly, predicted results for the radius of the supercoils (Fig. 4) show only a small difference between the asymptotic result [Eq. (11)] and the exact result of solving $\nabla\mathcal{G} = 0$. Finally, comparing Eqs. (16) and (17), one sees that

$$M \simeq \frac{2g(f)}{3\pi g'(f)}\, q. \tag{18}$$

This recovers a formula first discussed in Ref. [14] and which has been noted to describe experimental data for DNA torque [1].

In the computations presented in Ref. [5], a scaling factor of $\chi = 0.42$ in the effective charge ν [thereby using $\nu^\star = \chi\nu(a)$] plus a value $a = 1.2$ nm were used in order to obtain good agreement with experiments. We note that, in our model, we have not had to resort to a nonstandard value of the DNA effective charge. We agree with the assertion of Refs. [5,7] that single-DNA twisting-pulling experiments provide a means to analyze DNA-DNA interactions. The electrostatic potentials in the literature are Debye-Huckel-like, i.e., decaying as $(e^{-\rho})/\rho$, where $\rho = |\boldsymbol{r} - \boldsymbol{r}'|$ is the distance between interacting charges at $\boldsymbol{r}$ and $\boldsymbol{r}'$, and they involve an effective charge that in turn depends on salt concentration. For example, Ubbink and Odijk [11] have used an effective charge $\nu^\star = \xi/L_B$ with ξ given in their Table 7 (see also [15]). In counterion condensation theory of polyelectrolytes [16], the interaction energy also takes the same form as in Eq. (2), but with a salt-concentration-independent effective charge $\nu^\star = [1/(bL_B) - 1/(2L_B^2)]^{1/2} = 0.46$ for DNA in water solution [7,17]. The amplitude of the DNA-DNA interaction potential is sensitive to precisely where the charges are placed relative to the center of the double helix. This might explain the low values of effective charge inferred in Ref. [5]. Effective charges used by different authors are compared in Ref. [13].

Finally, we note that if the electrostatic-elastic theory were complete, then the rescaled slopes and torques in Figs. 2 and 3 would take on the value 1. While this limit is approached at high forces, at lower forces, there is disagreement, particularly in the case of the torques (Fig. 3). This effect is in part due to polymer confinement entropy [3], neglected here but which becomes important at low forces. There are also uncertainties about the measured low-force torque; the analysis of Ref. [1] required an estimate of torque as a boundary condition for integration of a thermodynamic "Maxwell relation" [18]. A more complete discussion of the model of this paper including confinement entropy, finite-size plectonemic and small-loop domain effects, and the collapse transition is in preparation.

The experimental data from Ref. [1] were kindly provided in electronic form by Francesco Mosconi. Work at NU was supported by the U.S. NSF through Grants No. DMR-0715099 and No. PHY-0852130, by the Chicago Biomedical Consortium and the Searle Funds at The Chicago Community Trust, and by NIH-NCI Grant No. U54CA143869-01.

[1] F. Mosconi, J.-F. Allemand, D. Bensimon, and V. Croquette, Phys. Rev. Lett. **102**, 078301 (2009).
[2] J. F. Marko and E. D. Siggia, Science **265**, 506 (1994).
[3] J. F. Marko and E. D. Siggia, Phys. Rev. E **52**, 2912 (1995).
[4] J. F. Marko, Phys. Rev. E **76**, 021926 (2007).
[5] C. Maffeo, R. Schöpflin, H. Brutzer, R. Stehr, A. Aksimentiev, G. Wedemann, and R. Seidel, Phys. Rev. Lett. **105**, 158101 (2010).
[6] J. D. Moroz and P. Nelson, Proc. Natl. Acad. Sci. U.S.A. **94**, 14 418 (1997).
[7] N. Clauvelin, B. Audoly, and S. Neukirch, Biophys. J. **96**, 3716 (2009).
[8] J. F. Marko and E. D. Siggia, Macromolecules **28**, 8759 (1995).
[9] D. Stigter, J. Colloid Interface Sci. **53**, 296 (1975).
[10] J. A. Schellman and D. Stigter, Biopolymers **16**, 1415 (1977).
[11] J. Ubbink and T. Odijk, Biophys. J. **76**, 2502 (1999).
[12] J. Bednar, P. Furrer, A. Stasiak, J. Dubochet, E. H. Egelman, and A. D. Bates, J. Mol. Biol. **235**, 825 (1994).
[13] See supplemental material at http://link.aps.org/supplemental/10.1103/PhysRevLett.106.138104 for two additional figures.
[14] N. Clauvelin, B. Audoly, and S. Neukirch, Macromolecules **41**, 4479 (2008).
[15] A. Vologodskii and N. Cozzarelli, Biopolymers **35**, 289 (1995).
[16] G. S. Manning, J. Chem. Phys. **51**, 924 (1969).
[17] J. Ray and G. S. Manning, Langmuir **10**, 2450 (1994).
[18] H. Zhang and J. F. Marko, Phys. Rev. E **77**, 031916 (2008).